Polymorphic Phase Behavior of Unsaturated Lysophosphatidylethanolamines: A ^{31}P NMR and X-ray Diffraction Study†

C. P. S. Tilcock,* P. R. Cullis, and M. J. Hope
Department of Biochemistry, The University of British Columbia, Vancouver, British Columbia, Canada V6T 1W5
S. M. Gruner
Department of Physics, Princeton University, Princeton, New Jersey 08544
Received August 5, 1985

ABSTRACT: The polymorphic phase behavior of aqueous dispersions of 1-oleoyl-, 1-linoleoyl-, and 1-linolenoyl-*sn*-3-glycerophosphoethanolamine (1-C18:1_c-PE, 1-C18:2_c-PE, and 1-C18:3_c-PE, respectively) has been investigated by ^{31}P NMR, small-angle and wide-angle X-ray diffraction, and freeze–fracture techniques in response to changes in temperature and pH. Between −20 and 0 °C at pH 7, NMR and X-ray data indicate that 1-C18:1_c-PE adopts a lamellar phase. Above 20 °C, the X-ray diffraction from 1-C18:1_c-PE reveals no long-range lattice order, whereas the NMR data indicate lamellar structure to 90 °C. Freeze–fracture electron microscopy shows that 1-C18:1_c-PE at pH 8.2 forms closed multilamellar vesicles upon dispersion and also that large unilamellar vesicles produced by extrusion techniques (LUVETs) can be made from 1-C18:1_c-PE at pH 7. Such LUVETs can trap [^{3}H]inulin and support a K^+ diffusion potential for up to 4 h. At pH 8.5 and above, 1-C18:1_c-PE forms optically clear, fluid dispersions with NMR and X-ray characteristics consistent with a micellar (noninverted) phase structure. Attempts to prepare LUVETs from 1-C18:1_c-PE at pH 9 result in structures that can neither trap [^{3}H]inulin nor support a membrane potential. At temperatures below −10 °C at pH 7, both 1-C18:2_c-PE and 1-C18:3_c-PE form a lamellar phase whereas at temperatures of 20 °C and above, both lipids form optically clear, gellacious phases with NMR and X-ray characteristics consistent with a phase (such as inverted micellar) in which the phospholipid head groups are not in intimate contact with the bulk aqueous phase. For both 1-C18:2_c-PE and 1-C18:3_c-PE at 0 °C, there is X-ray and NMR evidence, respectively, of a hexagonal phase, putatively H_{II}, occurring as an intermediate in the lamellar–inverted phase transition.

Lysophospholipids, while quantitatively minority components of most biological membranes, have been suggested to serve regulatory functions in processes as diverse as membrane fusion (Lucy, 1978), electrophysiological function (Corr et al., 1982), inflammatory processes (Bruni, 1982), chemoattraction (Hoffman et al., 1982), protein self-association (Smith, 1982), and ion transport (Wiswedel et al., 1982) as well as being implicated in certain pathological conditions (Edgar et al., 1982). Involvement in such a variety of processes is presumably related to the different physiochemical properties of lysophospholipids as compared to their diacyl counterparts. The only lysophospholipids studied systematically to date have been lysophosphatidylcholines, certain of which are thought to adopt interdigitated lamellar structures in the gel phase (Hauser et al., 1980; van Ecteld et al., 1981; Wu et al., 1982) and to form micellar structures at temperatures above the Krafft point (Reiss-Husson, 1967; Hauser et al., 1980; van Echteld et al., 1981; Wu et al., 1982; Ramsammy & Brockerhoff, 1982).

In this work, we present studies on the phase behavior of aqueous dispersions of three unsaturated 1-acyllysophosphatidylethanolamines (lyso-PE's) in response to changes in temperature and pH. It is shown that the phase behavior of unsaturated lyso-PE's differs considerably from that exhibited by lysophosphatidylcholines. In particular, it is shown that 1-oleoyl-PE (1-C18:1_c-PE) does not form micelles between pH 7 and 8.2 but rather adopts a lamellar configuration and can form closed vesicular structures. At higher pH values, this lyso-PE undergoes a transition from a lamellar to a micellar or hexagonal H_I phase. The more unsaturated lyso-PE's, 1-linoleoyl-PE (1-C18:2_c-PE) and 1-linolenoyl-PE (1-C18:3_c-PE), adopt a lamellar phase at low temperatures and undergo a transformation to an inverted (possibly micellar) phase at higher temperatures. This transition apparently occurs via a hexagonal H_{II} intermediate.

Materials and Methods

Lipid Synthesis. Dioleoylphosphatidylethanolamine, dilinoleoyl-PE, and dilinolenoyl-PE were synthesized and purified as described previously (Tilcock & Cullis, 1982). Lyso-PE's were derived from their respective diacyl-PE's by phospholipase A_2 hydrolysis as follows. Typically, 1 g of diacyl-PE was dissolved to clarity in 100 mL of analar-grade diethyl ether to which was added 20 mL of 0.5 M tris(hydroxymethyl)-aminomethane hydrochloride (Tris-HCl) (pH 7.4), 20 mL of 2 mM $CaCl_2$, and 50 mg of *Crotalus adamanteus* venom (Sigma). The reaction vessel was flushed with nitrogen and sealed, and the mixture was stirred vigorously at room temperature in the dark. After 24–36 h, complete conversion to the lyso derivative occurred as evidenced by thin-layer chromatography [$CHCl_3$/MeOH/25% NH_3/H_2O (90:54:5.7:5.3 v/v); silica gel 60 precoated plates, Merck]. The majority of the ether was removed by rotary evaporation and the aqueous phase extracted 3 times with 4 volumes of $CHCl_3$/MeOH (2:1 v/v). The extracts were pooled and concentrated to oils. Lyso-PE's were purified (>98%) by preparative liquid chromatography using a Waters Prep-500 LC unit with silica as support and $CHCl_3$/MeOH/H_2O (60:30:3 v/v) as eluant. Final purification was achieved by chromatography on CM-

†This work was supported by the Medical Research Council of Canada. P.R.C. is an MRC Scientist. S.M.G. is supported by National Institutes of Health Grant GM32614 and DOE Contract DEAC02-76EV03120.

0006-2960/86/0425-0816$01.50/0

cellulose (Whatman) employing a continuous gradient of 0–30% MeOH/$CHCl_3$. Lyso-PE's were characterized as 1-acyl-*sn*-3 conformers on the basis of ^1H NMR (Lammers et al., 1978) and by the absence of hydrolysis products upon reaction with purified phospholipase A_2. Lyso-PE's were greater than 99% pure with respect to lipid phosphorus as determined by phosphorus analysis following two-dimensional thin-layer chromatography and were greater than 99% pure with respect to their designated fatty acids as determined by gas chromatography of their methyl esters.

Nuclear Magnetic Resonance. Lipids (30–60 mg) were dispersed in 0.8 mL of 10 mM Tris-HCl, 100 mM NaCl, 2 mM ethylenediaminetetraacetic acid (EDTA), and 10% v/v ^2H_2O, pH 7, by vigorous vortex mixing at room temperature. Where applicable, Mn^{2+} was added as aliquots from a 1 M stock solution of the chloride salt. Variation in pH was accomplished by addition of aliquots of 10 mM HCl or NaOH. Spectra were accumulated by using a Bruker WP-200 spectrometer operating at 81 MHz for ^{31}P for up to 1000 transients employing a 0.8-s interpulse delay, 7-μs 90° radio-frequency pulse, and 20-kHz sweep width in the presence of broad-band proton decoupling. An exponential multiplication corresponding to 50-Hz line broadening was applied to the free induction decay prior to Fourier transformation.

Freeze–Fracture Electron Microscopy. Aliquots of samples were mixed with 25% (v/v) glycerol to prevent freeze damage. The samples were quenched from 20 °C by plunging into liquid freon and fractured at −110 °C by employing a Balzers BAF 400 apparatus. Micrographs were obtained by using a Phillips 400 electron microscope.

Preparation of 1-C18:1$_c$-PE Large Unilamellar Vesicles Produced by Extrusion Techniques (LUVETs). The procedure of Hope et al. (1985) was used with slight modifications. 1-C18:1$_c$-PE (20 mg/mL) was dispersed by extensive vortex mixing at room temperature in 169 mM potassium glutamate (KGlu) and 20 mM *N*-(2-hydroxyethyl)piperazine-*N*′-2-ethanesulfonic acid (HEPES), pH 7, in either the absence or the presence of 20 μCi of [^3H]inulin (NEN). The translucent, flocculant dispersion was then passed twice through two stacked 0.1-μm pore size filters (Nuclepore Corp.) at 300–350 lb/in.^{2} and then a further 10 times through two new stacked 0.1-μm filters at 100–150 lb/in.^{2}. The resulting dispersion was translucent with no evidence of flocculation for up to 8 h at room temperature.

Determination of Trapped Volume. 1-C18:1$_c$-PE LUVETs (2 mL) prepared in the presence of [^3H]inulin were loaded onto a 20-mL Ultrogel (LKB AcA-34) column and the vesicles eluted with 169 mM KGlu and 20 mM HEPES, pH 7, in order to separate free from entrapped inulin. Ultrogel was used in preference to Sephadex-G50 due to binding of PE to the latter, resulting in poor recoveries. Aliquots of the eluted material were assayed for lipid phosphorus (Bottcher et al., 1961), and entrapped inulin was estimated by using an LKB-Wallac 1217 Rackbeta scintillation counter and ACS (Amersham) scintillant. Trapped volumes are expressed as microliters of trapped volume per micromole of phospholipid.

Establishment and Measurement of Membrane Potentials. 1-C18:1$_c$-PE LUVETs were prepared in 169 mM KGlu/20 mM HEPES, pH 7. The untrapped buffer was exchanged for a NaCl buffer by passage through an Ultrogel column preequilibrated with 150 mM NaCl/20 mM HEPES, pH 7; the eluant was the same buffer. Membrane potentials were measured by determining the distribution of tetra[^3H]-phenylphosphonium bromide (TPPBr) (NEN, Canada); 2 μCi of TPPBr was added to 2 mL of LUVETs. A 100-μL sample was immediately removed, untrapped TPPBr was removed by low-speed centrifugation (500*g*, 2 min) through a 1-mL packed column of Sephadex-G50, and the eluate was sampled for phosphorus analysis and scintillation counting. The LUVET preparation was divided into two fractions, to one of which was added valinomycin (1 μg/μmol of phospholipid) and a 100-μL aliquot removed immediately for centrifugation and analysis as before. Samples were removed at intervals for up to 4 h. Knowledge of the trap volume enables calculation of the relative concentrations of probe inside and outside of the LUVETs, and, by application of the Nernst equation, membrane potentials may be calculated. See Hope et al. (1985) for further details.

X-ray Diffraction. Nickel-filtered Cu Kα (λ = 1.54 Å) X-rays were generated on a Rigaku RU-200 microfocus rotating anode generator equipped with a 0.2 × 2 mm microfocus gun. X-rays were collimated and focused by using single Franks mirror optics and slits (Gruner, 1977). Two-dimensional diffraction patterns were recorded by using film or the Princeton SIV-TV area detector (Reynolds et al., 1978) and reduced to one-dimensional scans by radial integration over ±5–20° areas as described elsewhere (Tilcock et al., 1984).

Specimens for X-ray diffraction were prepared by mixing lipids and buffer (see Nuclear Magnetic Resonance) in a 3:1 weight ratio. The resulting dispersion was loaded into either 1.5-mm acid-cleaned glass X-ray capillaries or a diffraction cell consisting of a 1-mm thick neoprene washer with 12.5-μm mylar windows. These were placed in a computer-controlled thermostated copper jacket on the X-ray specimen stage. The thermal accuracy was ±1 °C. Small-angle diffraction repeats are ±0.05 Å, and wide-angle repeats are ±0.1 Å. Typical X-ray exposure times were 2 min.

RESULTS

Figure 1 shows ^{31}P NMR spectra for aqueous dispersions of 1-C18:1$_c$-PE at pH 7 between −20 and 90 °C. All spectra correspond to an axially symmetric partially averaged motion on the NMR time scale, consistent with a lamellar configuration for the ensemble (Seelig, 1978; Hemminga & Cullis, 1982; Smith & Eikel, 1984). Micelles, or inverted micelles, would be expected to give rise to narrow ^{31}P NMR spectra indicative of isotropic motional narrowing due to the effects of rapid tumbling of the micelle in suspension and lateral diffusion of the lipids within the micelle. For 1-C18:1$_c$-PE at pH 7, such narrow resonances were never observed (Figure 1), suggesting that 1-C18:1$_c$-PE does not form small micelles at temperatures above the chain melting point. This is in marked contrast to the behavior of lysophosphatidylcholines (lyso-PC's) (Reiss-Husson, 1967; van Echteld et al., 1981; Ramsammy & Brockerhoff, 1982). From Figure 1, it is noted that the effective chemical shift anisotropy (CSA_{eff}) for 1-C18:1$_c$-PE above 20 °C is approximately −12 ppm as compared to −45 ppm for di-C18:1$_c$-PE in the liquid-crystalline state (Cullis & de Kruijff, 1979).

X-ray diffraction patterns (Figure 2) of 1-C18:1$_c$-PE dispersions (25% w/w lipid) also indicate that the system is lamellar at low temperatures. The presence of discrete ice reflections (Figure 2) indicates excess bulk water in the specimen. The small-angle X-ray scatter (SAXS) is dominated by 5 orders, indicative of an overall lamellar organization with a 47.4 ± 0.5 Å repeat. The wide-angle X-ray scatter (WAXS) is remarkable in that it consists of a series of closely spaced rings indicative of electron density repeats clustered mainly between 4 and 5.6 Å. These may arise from an in-plane (i.e., two-dimensional) crystalline organization of the lipids (Chang & Epand, 1983). Note, however, that the ^{31}P NMR

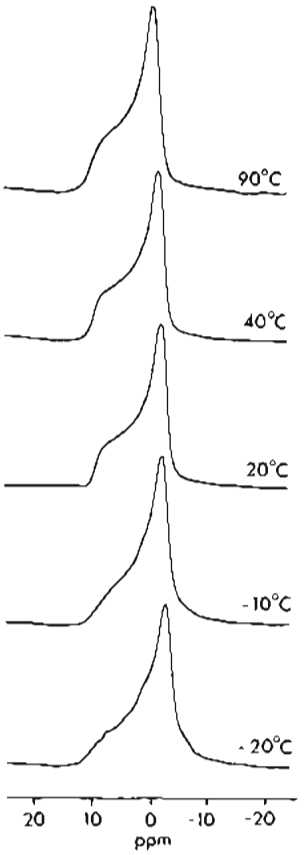

FIGURE 1: 81-MHz ^{31}P NMR spectra of aqueous dispersions of 1-C18:1_c-PE at pH 7 between −20 and 90 °C.

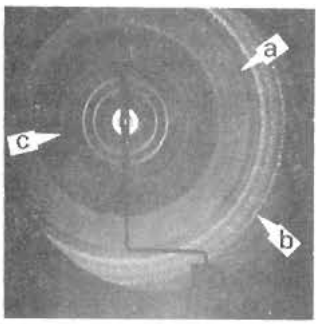

FIGURE 2: Diffraction pattern from a roughly 20% (w/w) dispersion of 1-C18:1_c-PE. The equidistantly spaced rings near the center ("c") are from a 47.7-Å lamellar lattice. The three finely speckled rings at the right periphery ("b") are from ice at 3.90, 3.67, and 3.44 Å. Note the series of closely spaced rings ("a") between the lamellar and ice reflections. This is an 11-h exposure with a 74.4-mm specimen to film distance.

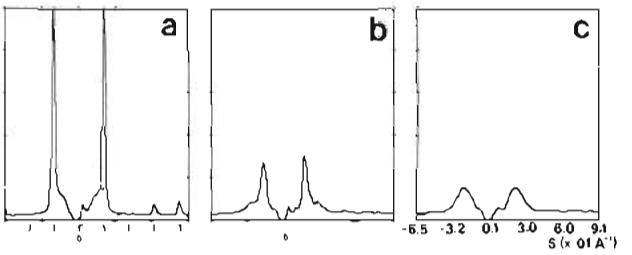

FIGURE 3: Small-angle X-ray scattering (SAXS) intensity (arbitrary units) from a 25% w/w dispersion of 1-C18:1_c-PE vs. $s = (\sin 2\theta)/\lambda$ (in units of 0.01 $Å^{-1}$) where 2θ is the scattering angle and $\lambda = 1.54$ Å is the Cu Kα X-ray wavelength. For Figures 3, 10, and 11, the zero angle of scatter (behind the beam stop shadow) is indicated by a zero below the abscissa. Equidistantly spaced tick marks indicate the expected peak positions of a lamellar lattice, and nonequidistantly spaced tick marks are for a hexagonal lattice. (a) −9 °C, lamellar basis = 47.6 Å; (b) 1 °C, largest peak corresponds to 58 Å; (c) 11 °C, peaks correspond to approximately 45 Å. Exposure times were 300 s.

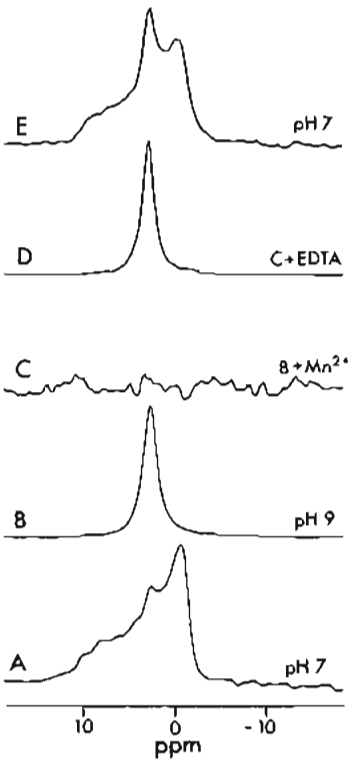

FIGURE 4: 81-MHz ^{31}P NMR spectra of a single aqueous dispersion of 1-C18:1_c-PE at 20 °C: (A) at pH 7; (B) at pH 9; (C) $MnCl_2$ was added to (B) to a final concentration of 2 mM; (D) EDTA was added to a final concentration of 5 mM; (E) the pH of the sample was lowered to pH 7.

spectrum at −20 °C (Figure 1) is not a typical rigid-lattice spectrum, suggesting that while at −20 °C the acyl chains are highly ordered, the phosphorylethanolamine moiety retains much of the motional freedom available at higher temperatures.

The thermal behavior of the SAXS of 1-C18:1_c-PE is shown in Figure 3. The pattern that was observed at −24 °C (Figure 2) changes little up to 9 °C (Figure 3a), consistent with the NMR results (Figure 1). At 1 °C (Figure 3b), the SAXS is no longer readily indexed as a single lamellar lattice. The corresponding WAXS (not shown) is now a broad, nearly featureless hump, indicative of melted acyl chains. Finally at 10 °C, the SAXS (Figure 3c) simply indicates a weak broad ring with a peak at roughly 45 Å; this is an unsampled diffraction pattern of the type expected in the absence of a regular lattice. Either micelles or uncorrelated lamellae could conceivably yield such a diffraction pattern. The SAXS remains qualitatively the same to at least 80 °C; thus, the high-temperature (10–80 °C) SAXS neither contradicts nor supports the ^{31}P NMR phase assignment as lamellar.

Support for the NMR interpretation as lamellar at higher temperatures comes from a variety of other sources. At high pH, there should be a deprotonation of a phosphorylethanolamine head group resulting in a net negative charge for the head group, thereby increasing the head-group repulsion and thus leading to a larger effective head-group area per molecule. As previously discussed (Israelachvili et al., 1976; Cullis & de Kruijff, 1979; Gruner et al., 1985), this would favor the formation of hexagonal H_I or micellar structures. The effect of variation of pH upon the polymorphic phase behavior of 1-C18:1_c-PE is illustrated in Figure 4. At pH 7, the dispersion was particulate. However, at pH 8.5 and

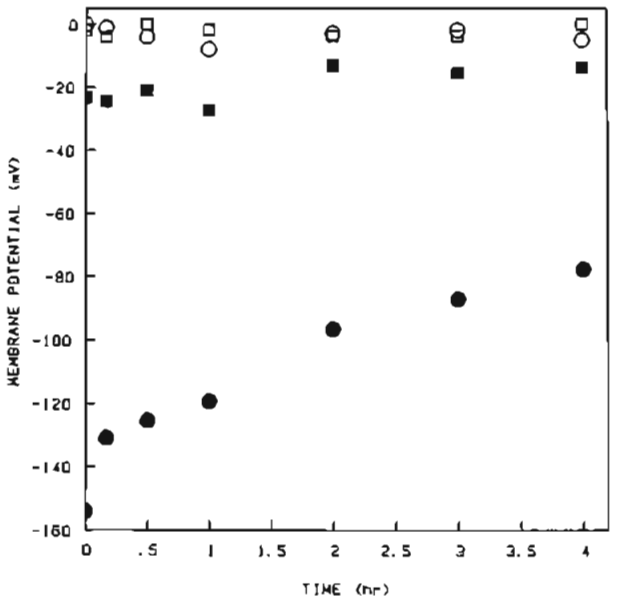

FIGURE 5: Time course at 20 °C of the membrane potential in 1-C18:1$_c$-PE LUVETs on application of a K^+ in/Na^+ out chemical gradient (see Materials and Methods for details) for LUVETs prepared at pH 7 (●) plus valinomycin or [■] minus valinomycin and at pH 9 (○) plus valinomycin or [□] minus valinomycin.

above, the dispersion was optically clear, and the corresponding ^{31}P NMR spectrum (Figure 4B) shows a narrow resonance indicative of isotropic motional averaging on the NMR time scale, suggesting that the state at pH 8.5 and above may consist of micelles or (short) H_I tubes.

Since both noninverted and inverted micelles are expected to yield isotropic motional averaging, we added Mn^{2+}, which acts as a broadening agent, to the 1-C18:1$_c$-PE dispersion at pH 9. If the lipid dispersion consisted of inverted micelles, then the head groups of the lipid would not be readily accessible to the Mn^{2+}, and thus their signal would not be readily quenched. However, it was observed (Figure 4C) that the addition of 2 mM Mn^{2+} fully quenched the ^{31}P NMR signal of a pH 9 dispersion within 5 min, the time required for signal accumulation. The subsequent addition of 5 mM EDTA led to the reestablishment of the isotropic resonance observed prior to the addition of Mn^{2+}. Subsequent reduction of the pH to 7 gave rise to a translucent dispersion with an anisotropic line shape similar to that shown in Figure 1.

Micelles or H_I systems would not be expected to contain a substantial entrapped aqueous volume. Therefore, 1-C18:1$_c$-PE was dispersed at pH 7 and 9 in the presence of [^{3}H]inulin via the LUVET protocol (Hope et al., 1985) which is known to produce vesicles with diacyl lipids. Free inulin was removed by chromatography on an agarose gel (see Materials and Methods) and lipid-associated entrapped inulin assayed by scintillation counting. At pH 7, three independent experiments gave an entrapped volume of 1.5 ± 0.1 μL/μmol of phospholipid, values comparable to those obtained with diacylphosphatidylcholines. At pH 9, however, no lipid-associated counts above background were detected. These results are consistent with structures at pH 7 that possess an entrapped volume and micellar (noninverted) structures at pH 9. Figure 5 shows that LUVETs prepared from 1-C18:1$_c$-PE at pH 7 are capable of developing and holding a K^+ diffusion potential in the absence and presence of valinomycin whereas at pH 9, no membrane potential could be established.

Graphic illustration of the macroscopic structures adopted by 1-C18:1$_c$-PE at pH 8.2 and 7 is given in Figure 6. Freeze–fracture electron microscopy shows that dispersions

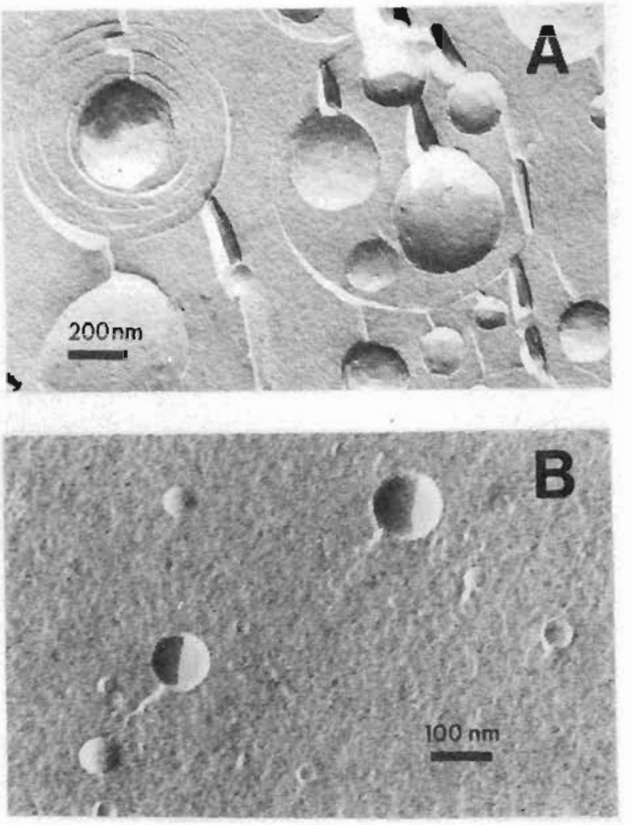

FIGURE 6: Freeze–fracture electron micrographs of (A) a 1-C18:1$_c$-PE vortex-shaken dispersion at pH 8.2 and (B) 1-C18:1$_c$-PE LUVETs (see Materials and Methods) at pH 7.

of 1-C18:1$_c$-PE at pH 8.2 (Figure 6A) form closed vesicular structures characterized by large, irregular interlamellar separations and a high degree of cross-fracturing. Such irregular bilayer packing provides an immediate explanation of the unsampled X-ray diffractions exhibited by 1-C18:1$_c$-PE at higher temperatures (Figure 3). Figure 6B shows the unilamellar nature of LUVETs produced at pH 7 and, together with Figure 6A, clearly demonstrates that 1-C18:1$_c$-PE in isolation adopts a lamellar phase between pH 7 and 8.2 at room temperature in full support of the ^{31}P NMR interpretation.

The effect of pH variation on the polymorphic phase behavior of an equimolar mixture of di-C18:1$_c$-PC and 1-C18:1$_c$-PE is shown in Figure 7. At pH 7, the equimolar mixture exhibits a spectrum corresponding to a superposition of the asymmetric line shapes expected of diC18:1$_c$-PC in a lamellar phase (Cullis & de Kruijff, 1979) and also from 1-C18:1$_c$-PE. Note that the value and sign of the CSA_{eff} of the 1-C18:1$_c$-PE component are very similar to those observed in isolation (Figure 1), indicating that the small CSA_{eff} is an intrinsic property of the lyso-PE rather than a consequence of the macroscopic averaging environment. Increasing the pH to 9.3 leads to the appearance of an isotropic component in the spectrum whereas at pH 10.4, the only spectral feature was a resonance indicative of isotropic motional averaging. Since di-C18:1$_c$-PC adopts a lamellar phase at pH 10.4 (Figure 7D), we interpret Figure 7C to indicate that at pH 10.4 di-C18:1$_c$-PC and 1-C18:1$_c$-PE are well mixed because there is no evidence of a (extended) lamellar component in the spectrum (Figure 7C). The other possibility, that Figure 7C represents isotropic resonances from small phosphatidylcholine vesicles superimposed upon isotropic resonances from micellar-phase 1-C18:1$_c$-PE, may also be discounted, because there is a small but resolvable difference in the chemical shift for

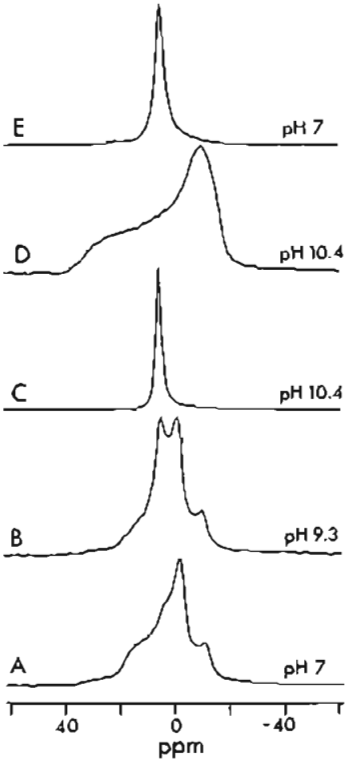

FIGURE 7: 81-MHz ^{31}P NMR spectra of a single aqueous dispersion of a di-C18:1_c-PC/1-C18:1_c-PE (1:1) mixture at 20 °C and at (A) pH 7, (B) pH 9.3, and (C) pH 10.4. Spectrum D is from di-C18:1_c-PC alone at pH 10.4. Spectrum (E) corresponds to sample C, but after the pH was lowered from 10.4 to 7.

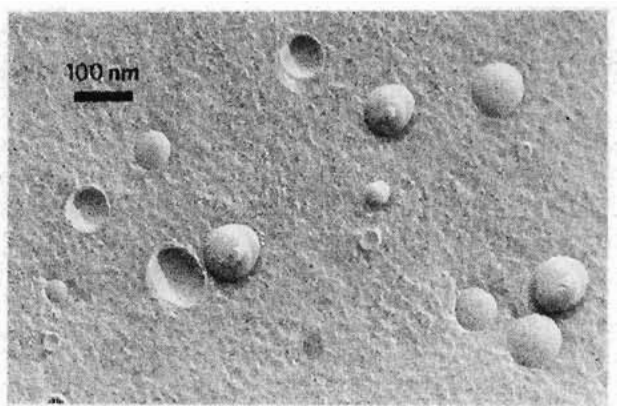

FIGURE 8: Freeze-fracture electron microscopy of a di-C18:1_c-PC/1-C18:1_c-PE (1:1) mixture dispersed at pH 7 and then raised in pH to 10.4 and back to 7.

those two lipid systems which would have been clearly detectable in the spectrum. It is of interest that decreasing the pH to 7 from 10.4 did not result in reestablishment of the original spectral line shape, but rather an isotropic resonance was observed. Figure 8 clearly demonstrates that this signal arises from the presence of vesicles, apparently uniformly unilamellar.

Figure 9 shows the ^{31}P NMR spectra obtained for 1-C18:2_c-PE (A) and 1-C18:3_c-PE (B) between −20 and 90 °C. Below 0 °C, both lipids give rise to spectra indicative of an overall lamellar organization by analogy with the previous findings for 1-C18:1_c-PE. Again, reduced CSA_{eff} compared to diacyl-PE's is observed. The SAXS from 1-C18:2_c-PE and 1-C18:3_c-PE are shown in Figures 10 and 11, respectively. For both lipids at low temperatures, the SAXS is dominated by a strong ring at roughly 44 Å. Two weak higher orders are also visible at multiples of this spacing, suggesting a lamellar

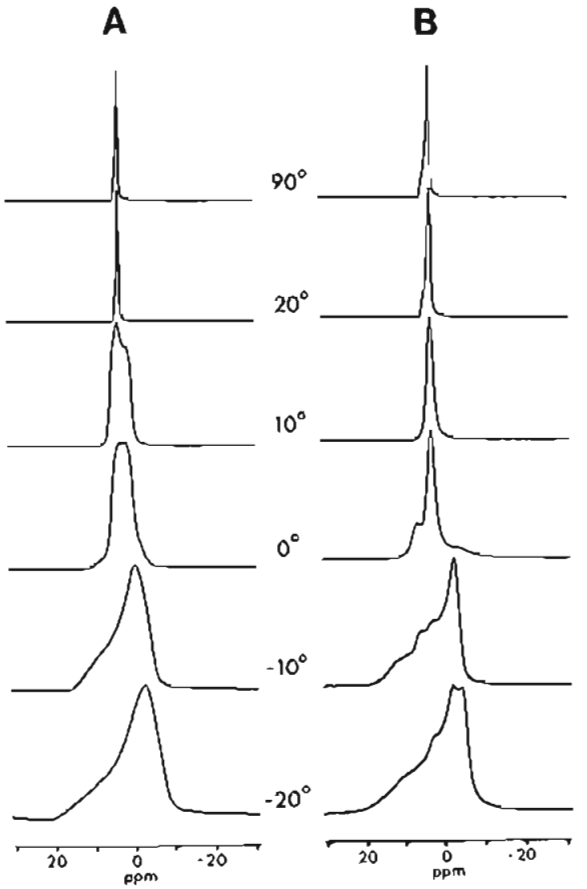

FIGURE 9: 81-MHz ^{31}P NMR spectra for aqueous dispersions of (A) 1-C18:2_c-PE and (B) 1-C18:3_c-PE at pH 7 between −20 and 90 °C.

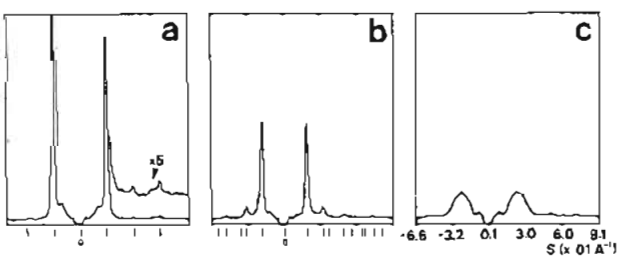

FIGURE 10: SAXS intensity vs. scattering angle for a 25% (w/w) dispersion of 1-C18:2_c-PE. See caption for Figure 3. (a) −9 °C, lamellar basis = 44.7 Å; (b) 0 °C, hexagonal basis = 61.5 Å; (c) 6 °C, peaks correspond to approximately 42 Å. Exposure times were 300 s.

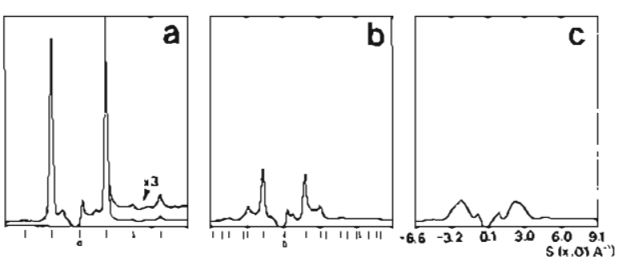

FIGURE 11: SAXS intensity vs. scattering angle for a 25% (w/w) dispersion of 1-C18:3_c-PE. See caption for Figure 3. (a) −19 °C, lamellar basis = 43.9 Å; (b) 0 °C, hexagonal basis = 65.6 Å; (c) 10 °C, peaks correspond to approximately 44 Å. Exposure times were 300 s.

organization, consistent with the NMR interpretation. A weak ring of unknown origin at 66–69 Å is also present in the patterns which does not index readily with the other orders. For 1-C18:2_c-PE at 0 and 10 °C, the ^{31}P NMR spectra (Figure 9) indicate the presence of at least two structures with different

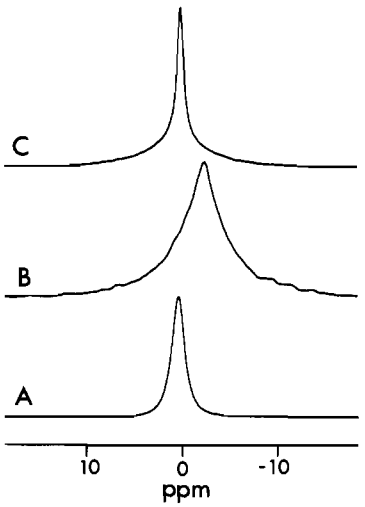

FIGURE 12: 81-MHz ^{31}P NMR spectra from 1-C18:2_c-PE at 20 °C at (A) pH 7 and (B) plus $MnCl_2$ to a final concentration of 2 mM. (C) Sample as in (B) plus EDTA to a final concentration of 5 mM.

degrees of motional averaging. For 1-C18:3_c-PE at 0 °C, the NMR spectrum is comprised of a strong isotropic component superimposed upon a weaker line shape with reversed asymmetry as compared to the lamellar line shape (Figure 1), which may be indicative of a hexagonal phase, H_I or H_{II}, by analogy with previous findings for diacyl lipids (Cullis & de Kruijff, 1979). For both 1-C18:2_c-PE and 1-C18:3_c-PE at 0–1 °C, the SAXS no longer indexes to a lamellar lattice (Figures 10b and 11b) but instead is best fit by a hexagonal lattice, consistent with the NMR interpretation. This X-ray indexing must be accepted cautiously, however, since it is based on the positions of the very few peaks visible in the diffraction patterns. Finally at higher temperatures, the SAXS is reduced to a single, broad, weak ring indicative of unsampled diffraction. Such diffraction could arise from either micelles or uncorrelated bilayers. The corresponding NMR spectra at 20 °C and above (Figure 9) show narrow, near-isotropic, resonances consistent with micellar (inverted or noninverted) structures.

It is of note that the phases exhibited by 1-C18:2_c-PE and 1-C18:3_c-PE, above 10 °C, were both transparent and highly gellacious in texture, whereas for 1-C18:1_c-PE, the high-temperature phase was transparent and fluid. In order to determine whether or not the phase was inverted, we examined the ^{31}P NMR spectra of 1-C18:2_c-PE in the presence of added Mn^{2+}. Figure 12 shows that upon addition of $MnCl_2$ to a final concentration of 2 mM, the NMR signal was considerably broadened but not eliminated in the 5-min period between addition of Mn^{2+} and spectral acquisition. In fact, these broad resonances persisted for at least 1 h after addition of Mn^{2+}. This suggests that the lipid head groups are relatively inaccessible to the added Mn^{2+}, a finding consistent with an inverted structure for the phase.

In order to better examine the hexagonal phase exhibited by 1-C18:3_c-PE at 0 °C (Figure 9), we undertook a time course measurement where a sample of 1-C18:3_c-PE, initially at −20 °C, was heated rapidly to 0 °C and then ^{31}P NMR spectra were accumulated over successive 50-s periods. The results are shown in Figure 13. Over the first 50 s, the NMR spectrum indicates the coexistence of three structures with different motional averaging properties: lamellar (indicated by SAXS data, Figure 11a), hexagonal (suggested by SAXS data, Figure 11b), and isotropic. Between 150 and 300 s after the temperature jump, the hexagonal component was the dominant spectral feature whereas after 400 s the isotropic component dominated. After 500 s, a spectrum was obtained that was virtually identical with that shown in Figure 9 at 0 °C.

Discussion

This study represents the first systematic investigation of the polymorphic phase properties of unsaturated lysophosphatidylethanolamines. It is clear that the structural preferences exhibited by these compounds on hydration differ significantly from their lysophosphatidylcholine counterparts. Two features of interest concern the NMR and other characteristics exhibited by the 1-C18:1_c-PE species and the reasons for the different phase structure adopted by lyso-PE's of varying unsaturation.

The ^{31}P NMR signal exhibited by the lamellar 1-C18:1_c-PE dispersions exhibits the usual asymmetric shape (with a low-field shoulder and high-field peak) associated with bilayer diacylphospholipid systems (Cullis & de Kruijff, 1979). The splitting between the shoulder and high-field peak (ΔCSA_{eff}) is, however, a factor of 3–4 less than that observed for diacyl-PE's. Similar effects have been observed for certain lysophosphatidylcholines (van Echteld et al., 1981, 1982) and may arise from increased local motion in the phosphate region or a different orientation of the methylene–phosphate methylene region with respect to the long axis of the molecule. In the absence of detailed crystallographic data or knowledge concerning order parameters in the glycerylphosphoethanolamine segment, the source of the reduced values of ΔCSA_{eff} cannot be readily ascertained. Two points that deserve emphasis, however, are that the identification of an asymmetric ^{31}P NMR spectrum with a low-field shoulder and high-field peak with bilayer structure remains valid even though ΔCSA_{eff} is reduced and that the permeability barrier presented by the 1-C18:1_c-PE bilayers is remarkably tight. In particular, the ability of the lysooleoyl-PE LUVETs to maintain a K^+ diffusion potential is comparable to that observed (Hope et al., 1985) for diacylphosphatidylcholines. This suggests that whatever the source of the increased motional averaging in the head group, the acyl chains are not markedly more disordered than in diacylphospholipid bilayer systems.

As well as providing graphic supportive evidence for the bilayer arrangement of 1-C18:1_c-PE dispersions, the freeze–fracture micrographs of these systems exhibit two other interesting features. The first concerns the somewhat irregular cleavage planes between the lyso-PE monolayers and the frequent observation of cross-fractures. These observations suggest that fractures through the middle of the lyso-PE bilayers are somewhat less favored than for diacylphospholipids, for example, which could be related to a certain measure of interdigitation between the acyl chains of opposed monolayers. This would be consistent with the observation that (crystalline) bilayers of lyso-PC are fully interdigitated with a corresponding reduction in bilayer thickness (Hauser et al., 1980). A second feature concerns the large and variable interlamellar spacings, observed for the multilamellar 1-C18:1_c-PE dispersions (Figure 8). This behavior explains the inability of X-ray techniques, which require regular, closely packed arrays, to determine the phase structure of these systems.

The phase preferences of the lyso-PE's are markedly different than for lyso-PC's, and it is of interest to examine the physical basis for this. There is now considerable evidence to support the view that the phase adopted by a given lipid is dictated by the dynamic molecular "shape" assumed on hydration. In particular, employing current nomenclature (Gruner et al., 1985), lipids such as unsaturated diacyl-PE's [which commonly adopt the hexagonal (H_{II}) phase] exhibit a "cone" shape where the area subtended by the head group

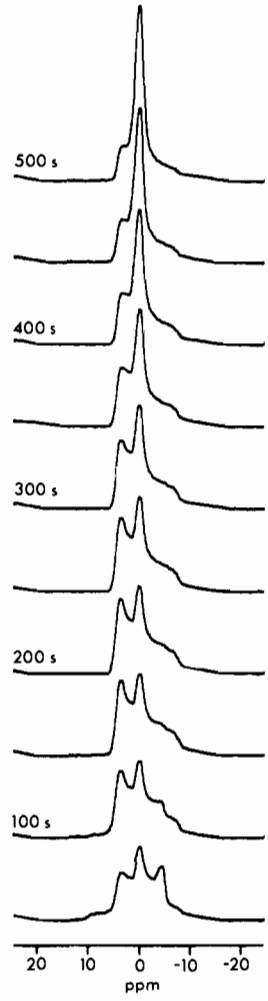

FIGURE 13: 81-MHz ^{31}P NMR spectra of 1-C18:3$_c$-PE at pH 7. 150 mg of lipid was dispersed in 20 mM HEPES and 150 mM NaCl, pH 7, and stored at −20 °C overnight. It was subsequently transferred to the NMR preequilibrated at −20 °C, the temperature was raised rapidly to 0 °C, and spectra were accumulated every 50 s over a period of 10 min. The time in seconds is given adjacent to every second spectrum.

is smaller than that subtended by the acyl chain. Alternatively, lipids preferring the micellar organization exhibit an "inverted cone" shape, whereas bilayer lipids may be considered to assume a relatively cylindrical geometry. This framework provides a simple qualitative explanation of the phase properties of the unsaturated lyso-PE's. Removal of an acyl chain from di-C18:1$_c$-PE to produce 1-C18:1$_c$-PE, for example, may be considered to result in a more cylindrically shaped molecule compatible with bilayer organization. Higher pH values, on the other hand, increase the electrostatic repulsion between PE head groups (due to deprotonation of the primary amine) and thus increase the effective head-group area. This is consistent with an increasing inverted cone shape of 1-C18:1$_c$-PE as the pH is raised above 9, giving rise to a micellar structure.

The phase behavior of the more unsaturated lyso-PE species (1-C18:2$_c$-PE, 1-C18:3$_c$-PE) is also broadly consistent with the shape hypothesis. In particular, the increased unsaturation of 1-C18:3$_c$-PE (as compared to 1-C18:1$_c$-PE) would be expected to produce an increased cone shape character. Similarly, an increase in temperature will increase the entropic splay of the acyl chains due to gauche–trans isomerization. Thus, the phase giving rise to the isotropic motion observed for 1-C18:2$_c$- and 1-C18:3$_c$-PE dispersions as the temperature is raised is most likely an inverted (e.g., inverted micellar) structure. For similar reasons, the hexagonal intermediate observed is most probably hexagonal H_{II}.

In summary, the results presented here show definitively that 1-C18:1$_c$-PE adopts the bilayer phase at pH 7, whereas at higher pH values a different, possibly micellar, structure is observed. More unsaturated species of lyso-PE exhibit behavior consistent with increased cone shape character. This behavior differs dramatically from that normally associated with lysophospholipids. In particular, it would not be expected that such compounds would exhibit lytic properties in membranes.

REFERENCES

Böttcher, C. J. F., van Gent, C. M., & Pries, C. (1961) *Anal. Chim. Acta 24*, 203–204.

Bruni, A. (1982) *Pharmacol. Res. Commun. 14*, 469–484.

Chang, A., & Epand, R. M. (1983) *Biochim. Biophys. Acta 728*, 319–324.

Corr, P. B., Synder, D. W., Lee, B. M., Gross, R. W., Keim, C. R., & Sobel, B. E. (1982) *Am. J. Physiol. 243*, 187–195.

Cullis, P. R., & de Kruiff, B. (1979) *Biochim. Biophys. Acta 559*, 339–420.

Edgar, D., Stosznajder, J., & Horrocks, L. A. (1982) *J. Neurochem. 39*, 1111–1116.

Gruner, S. M. (1979) Ph.D. Thesis, Princeton University, Princeton, NJ.

Gruner, S. M., Cullis, P. R., Hope, M. J., & Tilcock, C. P. S. (1985) *Annu. Rev. Biophys. Bioeng. 14*, 211–238.

Hauser, H., Guyer, W., Spiess, M., Pascher, I., & Sundell, S. (1980) *J. Mol. Biol. 137*, 265–282.

Hemminga, M. A., & Cullis, P. R. (1982) *J. Magn. Reson. 47*, 307–323.

Hoffman, R. D., Kligerman, M., Sundt, T. M., Aderson, N. D., & Shin, H. S. (1982) *Proc. Natl. Acad. Sci. U.S.A. 79*, 3285–3289.

Hope, M. J., Bally, M. B., Webb, G., & Cullis, P. R. (1985) *Biochim. Biophys. Acta 812*, 55–65.

Israelachvili, J. N., Mitchell, D. J., & Ninham, B. W. (1976) *J. Chem. Soc., Faraday Trans. 2, 72*, 1525–1568.

Lammers, J. G., Liefkens, T. J., Bus, J., & van der Meer, J. (1978) *Chem. Phys. Lipids 22*, 293–305.

Lucy, J. A. (1978) *Cell Surf. Rev. 5*, 267–304.

Ramsammy, L. S., & Brockerhoff, H. (1982) *J. Biol. Chem. 257*, 3570–3574.

Reiss-Husson, F. (1967) *J. Mol. Biol. 25*, 363–382.

Reynolds, G. T., Milch, J. R., & Gruner, S. M. (1978) *Rev. Sci. Instrum. 49*, 1241–1249.

Seelig, J. (1978) *Biochim. Biophys. Acta 515*, 105–140.

Smith, I. C. P., & Ekiel, I. H. (1984) in *Phosphorus-31 NMR. Principles and Application*, pp 447–475, Academic Press, New York.

Smith, R. (1982) *Biochemistry 21*, 2697–2701.

Tilcock, C. P. S., & Cullis, P. R. (1982) *Biochim. Biophys. Acta 684*, 212–218.

Tilcock, C. P. S., Bally, M. B., Farren, S. B., Cullis, P. R., & Gruner, S. M. (1984) *Biochemistry 23*, 2696–2703.

van Echteld, C. J. A. (1982) Ph.D. Thesis, State University of Utrecht, Utrecht, The Netherlands.

van Echteld, C. J. A., de Kruijff, B., Mandersloot, J. G., & de Gier, J. (1981) *Biochim. Biophys. Acta 649*, 211–220.

Verkleij, A. J. (1984) *Biochim. Biophys. Acta 779*, 43–64.

Wiswedel, I., Barnstrorf, U., Augustin, W., Holmuhamedov, E., Medvedev, B., & Evtodienko, Y. (1982) *Biochim. Biophys. Acta 688*, 597–604.

Wu, W., Huang, C., Conley, T., Martin, R. B., & Levin, I. A. (1982) *Biochemistry 21*, 5957–5961.